Bull Volcanol (2002) 64:31–39
DOI 10.1007/s00445-001-0180-3

RESEARCH ARTICLE

Graham Veitch · Andrew W. Woods

Particle recycling in volcanic plumes

Received: 22 April 2000 / Accepted: 11 September 2001 / Published online: 24 October 2001

Abstract We have developed a new theoretical model of an eruption column that accounts for the re-entrainment of particles as they fall out of the laterally spreading umbrella cloud. The model illustrates how the mass flux of particles in the plume may increase with height in the plume, by a factor as large as 2.5 because of this recycling. Three important consequences are that (1) the critical velocity required to generate a buoyant eruption column for a given mass flux increases, (2) the total height of rise of the column may decrease, and (3) we infer that in relatively wind-free environments, for eruption columns near the conditions for collapse, the recycling of particles may lead to an unsteady oscillating motion of the plume, which, in time, may lead to the formation of interleaved fall and flow deposits.

Introduction

Explosive volcanic eruptions can release large volumes of gas and hot ash over a sustained period (Sparks et al. 1997). These flows are initially dense, driven upwards by their momentum, but entrain air from the surroundings by a process of turbulent mixing. This entrainment produces a radial inward velocity field in the surroundings. If the plume entrains sufficient air, it may become buoyant before it runs out of momentum, and may then rise tens of kilometres, driven by its buoyancy, before spreading radially as an umbrella cloud. However, if the speed of the initial momentum-driven jet falls to zero before it becomes buoyant, it will collapse down the flanks of the volcano, forming pyroclastic flows. The transition between these two states is of key importance in assessing the hazards of the volcano (Carey and Sigurdsson 1987).

If the plume becomes buoyant, and an umbrella cloud is formed, it will spread initially as a gravity current, becoming wind-driven at large distances from the source (Carey and sparks 1986; Sparks et al. 1991). Particles will sediment from the cloud, and may be re-entrained into the rising plume by the radial inward velocity field generated by turbulent entrainment. In this paper, we consider the effects of this particle recycling on the dynamics of the plume and, in particular, on the conditions at which there is a transition from the formation of the eruption column to flow activity. We consider the idealised case of a plume rising in a wind-free environment, in which the proportion of solid material recycled into the plume will be maximised. This limit may be relevant for historic eruptions such as the Fogo A eruption in the Azores (Bursik et al. 1992) and illustrates the maximum effect of such re-entrainment.

The dynamics of volcanic eruption columns have been extensively studied (Wilson 1976; Woods 1988) using steady models of the flow that average over the timescale of turbulent fluctuations and neglect the effects of particle recycling. However, real eruption columns are highly turbulent unsteady flows, either because the properties of the magma at the vent may vary (Wilson et al. 1980) because of two-phase flow instabilities (Anilkumar et al. 1993), or because dynamical process in the atmosphere may lead to unsteady flow. Woods and Caulfield (1992) identified that non-linear mixing of air in the gas-thrust region may lead to an instability with a period given by the reciprocal of the atmospheric buoyancy frequency. Numerical experiments have demonstrated that unsteady flows may result from both the recycling of particles into the central jet from the collapsing eruption column and also because of complex transient dynamics of pyroclastic dispersion into the atmosphere (Neri and Dobran 1994).

Editorial responsibility: D. Dingwell

G. Veitch
Institute of Theoretical Geophysics, Department of Applied, Mathematics and Theoretical Physics, University of Cambridge, Silver Street, Cambridge, CB3 9EW, UK

A.W. Woods (✉)
B.P. Institute for Multiphase Flow, University of Cambridge, Madingley Rise, Madingley Road, Cambridge, CB3 0EZ, UK
e-mail: andy@bpi.cam.ac.uk
Tel.: +44-01223765702, Fax: +44-01223765701

Veitch and Woods (2000) reported that particle recycling may have a significant effect on the dynamics of an experimental Boussinesq plume in the laboratory. At the limit when the plume height is small compared with the ambient scale height, recycling may cause a steady plume to collapse. In this paper, we develop the modelling of Veitch and Woods (2000) for application to a volcanic eruption column by including the effects of heat transfer between solid and gas phases, and of pressure and density variations with height in the atmosphere.

A plume that recycles particles may tend to a steady state if the source conditions are constant over a time-scale longer than the recycling period. For particles with settling speeds in the range 1–10 m s^{-1}, and a plume height 1–10 km, we expect the recycling time to be comparable to the particle fall time, which will be of the order 100–10,000 s. If the eruption becomes oscillatory as a result of particle recycling, we expect the period of oscillation to scale with the particle fall time, as observed in laboratory experiments (Veitch and Woods 2000). The numerical simulations of Neri and Dobran (1994) reveal oscillations on a time-scale of 50 s, similar to the smaller end of the above range.

In the present work we examine the limit of steady-state plumes. Our models identify the different criteria for column formation for recycling and non-recycling plumes and this, in turn, identifies criteria under which steady source conditions may lead to unsteady plume behaviour.

In the next section, we develop a model of volcanic eruptions to describe the recycling of particles, which includes the essential thermodynamics of hot particle-laden plumes. We also discuss the dependence of particle fall speed on particle size and height, and the effect this has on particle re-entrainment. In the Numerical methods section we comment on the solution of the model, and in the Results we describe how particle recycling lowers the critical speed at which there is a transition from plume-forming eruptions to those that collapse to form pyroclastic flows. We also describe the effect of recycling on the height of the laterally spreading neutral intrusion that forms above a steady plume. In the Discussion we consider these results and their implications for volcanic eruptions.

Model

Following the approach of Morton et al. (1956), we work with the vertical fluxes of mass, πQ, momentum, πM and density deficit, πD (Table 1). However, for a plume with two components (one solid, one gas), we also need to describe the evolution of the particle fraction in the column.

We adopt the top-hat model (Morton 1959) for the plume in which the model plume speed ω, bulk density ρ, and solid mass fraction ø are functions of height alone inside some radius $r=b(z)$. The fluxes are then

$$Q = p(z)\, b^2(z)\, w(z) \tag{1}$$

Table 1 Definitions

Symbol	Meaning
C_D	Drag coefficient
D	Flux of density deficit/π in plume, $g(\rho_a - \rho)b(z)^2 w(z)^2$
F	Integration variable – see Eq. (26)
$H(r)$	Thickness of the laterally-spreading intrusion
M	Momentum flux/π in plume, $\rho(z)b(z)^2 w(z)^2$
Q	Mass flux/π in plume $\rho(z)b(z)^2 w(z)$
R	Gas constant
S	Shooting parameter related to plume height z_t – see Eq. (30)
T	Absolute temperature in plume
T_a	Absolute temperature in ambient
b	Plume radius at height z
c_p	Specific heat of gas at constant pressure
c_s	Specific heat of solid
g	Gravitational acceleration
h	Specific enthalpy in plume
h_a	Specific enthalpy in entrained material
p	Pressure
r	Radial distance from axis of plume
$r0$	Radius of 'corner' between plume and gravity current
r_t	Radial co-ordination in gravity current
u	Radial speed in laterally spreading intrusion
u_e	Entrainment speed
v	Settling speed of particles
w	Plume speed
x	Scaled height variable
z	Height
z_t	Height of radial intrusion
α	Entrainment coefficient
β	$(c_s - c_p)/c_p$
μ	Dynamic viscosity of air
ρ	Average density of plume
ρ_t	Average density at top of plume
ρ_a	Density of ambient
ρ_0	Density of ambient at z=0
ρ_e	Density of entrained material
ρ_s	Particle density
ø	Mass fraction of solid in plume
$ø_e$	Mass fraction of solid in ambient
$ø_{gc}(r)$	Particle mass fraction in gravity current
Subscript I	Initial value of quantity at source
Subscript t	Value of quantity at neutral height $z=z_t$

$$M = \rho(z)\, b^2(z)\, w^2(z) \tag{2}$$

$$D = g\left[\rho_a(z) - \rho(z)\right] b^2(z)\, w(z), \tag{3}$$

where $\rho(z)$ is the density of the ambient atmosphere.

The steady-state equations for conservation of mass and momentum are

$$\frac{dQ}{dz} = \frac{d}{dz}\left(\rho b^2 w\right) = 2bu_e\rho_e \tag{4}$$

$$\frac{dM}{dz} = \frac{d}{dz}\left(\rho b^2 w^2\right) = gb^2\left(\rho_a - \rho\right). \tag{5}$$

where ρ_e is the density of the entrained material (which will only be equal to ρ_a if no particles are entrained), and turbulent entrainment is parameterised by the entrainment speed u_e at $r=b$. In a non-Boussinesq plume, this speed is proportional to the mean upward speed in the plume, and to the square root of the density ratio between the plume and the ambient (Ricou and Spalding 1961):

$$u_e = \alpha w \left(\frac{\rho}{\rho_e}\right)^{1/2}, \tag{6}$$

where α is a constant of proportionality, which has been determined empirically to have value α=0.1 based on laboratory experiments (Morton et al. 1956).

We use the steady-flow energy equation (Shapiro 1953; Woods 1988) to describe the thermodynamics of the plume. In steady state, the net flux of enthalpy and kinetic and potential energy from any control volume is zero. We assume that the solid particles are sufficiently small that they remain in thermal equilibrium with the surrounding gas. This is valid for particles smaller than about 4 mm (Woods and Bursik 1991). With this assumption, the bulk density of the plume is related to the solid mass fraction ø, the density of solid ρ_s, the absolute temperature T and the pressure p by

$$\frac{1}{\rho} = \frac{\phi}{\rho} + \frac{(1-\phi)RT}{p}. \tag{7}$$

We also assume that when falling particles are re-entrained they have the temperature of the ambient atmosphere at that height. The specific enthalpy of the mixture is

$$h = [\phi c_s + (1-\phi)c_p]T + \frac{p\phi}{\rho_s} \tag{8}$$

where c_s and c_p are the specific heats of the solid particles and the gas at constant pressure. We can neglect the final term, $p\text{ø}/\rho_s$ provided that $\text{ø}/\rho_s << (1-\text{ø})RT/p$, which is always true in volcanic eruption columns, so

$$h \approx (1+\beta\phi)c_pT \tag{9}$$

where $\beta = c_s/c_p - 1$.

Similarly, the specific enthalpy of the material, with solid mass fraction ø_e and temperature T_a, which is entrained into the plume is

$$h_a = (1+\beta\phi_e)c_pT_a. \tag{10}$$

In the steady-flow energy equation, we neglect the kinetic energy of the entrained material, as the entrainment speed is much less than the speed of the plume. This leads to the relationship:

$$\frac{d}{dz}\left[\left(h+gz+w^2/2\right)Q\right] = (h_a+gz)\frac{dQ}{dz}. \tag{11}$$

We use Eq. (11) as a predictive equation for the enthalpy h, and derive a predictive equation for the density deficit D by noting that the enthalpy h is related to the temperature by Eq. (8) and, therefore, to the plume density by Eq. (7). We find that

$$\begin{aligned}\frac{1}{g}\frac{dD}{dz} = &\left[\frac{(1+\beta)\phi}{1+\beta\phi}\left(\frac{T}{T_a}-1\right)+\frac{1-\phi}{1+\beta\phi}\frac{w^2}{2c_pT_a}\right]\frac{dQ}{dz}\\ &+\left[\frac{1}{\rho}\frac{d\rho_a}{dz}-\frac{T(1-\phi)}{T_a}\frac{1}{p}\frac{dp}{dz}-\frac{1-\phi}{1+\beta\phi}\frac{9\rho_a}{c_pT_a\rho}\right]Q\\ &+\left[\frac{\rho_a}{\rho_s}+\frac{\beta(1-\phi)}{1+\beta\phi}-\frac{1+\beta}{1+\beta\phi}\frac{T}{T_a}\right]\frac{d}{dz}(Q\phi).\end{aligned} \tag{12}$$

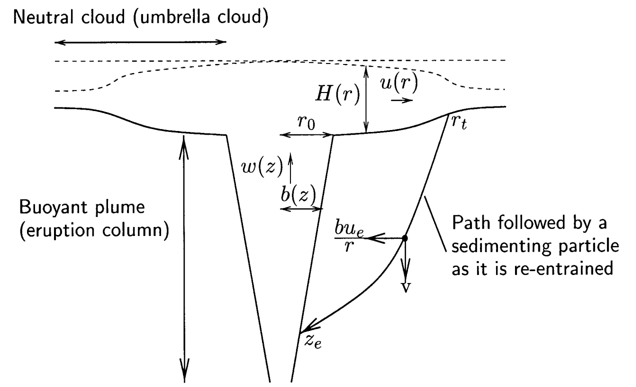

Fig. 1 Diagram illustrating the variables in the plume and region of particle fallout

In order to complete the model, we require to couple Eqs. (4), (5) and (12) with a description of the evolution of the particle fraction ø. This is discussed in the next section.

Fallout

Many volcanic plumes will rise tens of kilometres into the atmosphere before spreading radially as a neutral intrusion. The density of the atmosphere at this height will be much less than the density at sea level, and this may significantly increase the fall speed of the particles. Therefore, we extend the fallout model of Sparks et al. (1991) to include the variation in fall speed with height. The key variables are illustrated in Fig. 1.

We concentrate on the idealised case of an eruption with steady source conditions. If we consider a particle with settling speed $v(z)$ moving in the radially inward entrainment velocity field, the position (r, z) of the particle as it falls is given by

$$\frac{dr}{dt} = -u_e(z)\frac{b(z)}{r} \tag{13}$$

$$\frac{dz}{dt} = -v(z), \tag{14}$$

where $u(z)$ is the entrainment velocity at the edge of the plume at height z. If a particle that falls from the neutral cloud at radius r_t is re-entrained at height z_e above the ground, then r_t and z_e are related by the expression

$$r_t^2 = b^2(z_e) + \int_{z_e}^{z_t}\frac{2bu_e}{v}dz = b^2(z_e) + \int_{z_e}^{z_t}\frac{1}{\rho_e v}\frac{dQ}{dz}dz. \tag{15}$$

The mass flux of solid entrained above height z_e is therefore equal to the mass flux that sediments from the radial intrusion at distances $r<r_t$. We assume that the gravity current is well mixed, with particles sedimenting at their settling speed from the base of the turbulent layer (Martin and Nokes 1988; Sparks et al. 1991). The solid fraction in the gravity current, ø_{gc}, therefore satisfies

$$\frac{\partial}{\partial t}\left(rH\rho_{gc}\phi_{gc}\right)+\frac{\partial}{\partial r}\left(ruH\rho_{gc}\phi_{gc}\right)=-ru_t\rho_{gc}\phi_{gc}, \tag{16}$$

where ρ_{gc} is the bulk density of the gravity current at radius r from the axis, v_t is the particle settling speed at the neutral height, and H is the thickness of the gravity current.

In steady state, the mass flux in the gravity current, $ruH\rho_{gc}$ is approximately constant if the solid mass fraction is small. Equation (16), therefore, has the solution

$$Q_t\phi_{gc}(r)=Q_t\phi_t\exp\left[-\frac{\rho_t v_t}{Q_t}\left(r^2-r_0^2\right)\right], \tag{17}$$

where r_0=$b(z_t)$, ρ_{t1} Q_t, and $\o_t$ are the values of the density, mass flux and solid mass fraction at the top of the plume, height z=z_t. This is valid in the near field where the spreading cloud is well-mixed and coherent. The flux that falls out between r=r_0 *and* r=r_t is re-entrained in the region of the plume between z=z_e and z=z_t. Therefore, the increase in solid mass flux in the plume between these heights is

$$Q_t\phi_t-Q(z_e)\phi(z_e)=Q_t\left(\phi_t-\phi_{gc}(r_t)\right) \tag{18}$$

$$=Q_t\phi_t\left\{1-\exp\left[-\frac{\rho_t v_t}{Q_t}\left(r_t^2-r_0^2\right)\right]\right\}, \tag{19}$$

We set z=0 in Eq. (18) to show that the initial solid mass flux $Q_I\o_I$ is related to the solid mass flux at the plume top by

$$Q_I\phi_I=Q_t\phi_t\exp\left[-\frac{\rho_t v_t}{Q_t}\left(r_t^2-r_0^2\right)\right], \tag{20}$$

where Q_I is the mass flux and $\o_I$ is the solid fraction at the source. Using the expression for r_t in Eq. (15), the solid mass flux at any height in the plume is therefore related to the initial mass flux by the relationship

$$\begin{aligned}Q(z_e)\phi(z_e)=&\\ &Q_I\phi_I\exp\left[\int_0^{z_e}\frac{\rho_t v_t}{\rho_e v}\frac{1}{Q_t}\frac{dQ}{dz}dz+\frac{\rho_t v_t}{Q_t}\left(r_0^2-b(z_e)^2\right)\right]\\ &\approx Q_I\phi_I\exp\left[\int_0^{z_e}\frac{\rho_t v_t}{\rho_e v}\frac{1}{Q_t}\frac{dQ}{dz}dz\right],\end{aligned} \tag{21}$$

when the particle fall speed v_t is small compared with the velocity scale $Q_t r_t r^2_0$.

On small scales, where the fluid is incompressible, Eq. (21) implies that the flux of particles increases by a factor e≈2.71. However, if the fluid is compressible, the situation is more complex. Firstly, the decrease in pressure with height causes the ascending plume to decompress. As a result, the volume flux increases by more than would be predicted by entrainment alone. For a given ambient stratification, a larger volume flux will lead to a higher radial speed in the intrusion. In turn, this tends to disperse particles farther from the plume before they fall out, and thereby reduces the fraction of particles that is re-entrained.

This reduction in the fraction of particles that is re-entrained because of the effects of gas expansion may be partially offset by the increase of particle fall speed with height. Because the density of air decreases with height, the fall speed of the particles increases with height. As a result, particles tend to settle more rapidly from radial intrusions that spread at greater altitudes. As they fall into denser air, their fall speed decreases, allowing more time for entrainment. We calculate fall speeds of particles using the drag coefficients of Turton and Clark (1987) and an atmospheric density profile appropriate for mid-latitudes, as given by Woods (1988).

For small particles with radius a, which obey Stokes' law, the settling speed is

$$v=\frac{2\rho_s g a^2}{9\mu}. \tag{22}$$

The only variation of settling speed with height is through the variation of the dynamic viscosity μ with height. For pressures less than 20 atm, the dynamic viscosity of air is approximately proportional to the square root of its absolute temperature, and independent of the pressure (Kaye and Laby 1973). Our model atmosphere varies in temperature between from about 300 K at sea level to 230 K in the stratosphere, corresponding to a change in viscosity of around 14%. Although this variation may affect the details of the fall speed for each particle, we ignore it in considering the limiting behaviour, and treat the dynamic viscosity as a constant. This, in turn, implies that the settling speed is constant, and that the ratio of speeds in Eq. (21) is v_t/v=1.

At the other extreme, for large particles that have a constant drag coefficient, C_D≈1.0, the settling speed is

$$v=\left(\frac{2\rho_s g a}{3\rho_a}\right)^{1/2}. \tag{23}$$

In this case, the fall speed is independent of the viscosity, but inversely proportional to the square root of the ambient density. In Eq. (21), the speed ratio

$$\frac{v_t}{v(z)}=\left(\frac{\rho_a}{\rho_t}\right)^{1/2}>1. \tag{24}$$

This factor identifies that although large particles fall faster than small ones, they slow down as they fall, and hence are more likely to be re-entrained. To illustrate the maximum effect that recycling of particles may have, we therefore concentrate on the limit where all particles fall with inertial drag.

Numerical method

We use a shooting method to find a numerical solution to the system of ordinary differential Eqs. (4), (5), (12) and (21). For convenience in performing the integration, we introduce a new variable F such that

$$F=\int_0^{z}\frac{\rho_t v_t}{\rho_e v}\frac{1}{Q_t}\frac{dQ}{dz}dz, \tag{25}$$

so

$$\frac{dF}{dz} = \frac{\rho_t v_t}{\rho_e v} \frac{1}{Q_t} \frac{dQ}{dz}, \tag{26}$$

and from Eq. (21),

$$Q\phi = Q_I \phi_I \exp F. \tag{27}$$

Note that F has no simple direct physical interpretation, but is introduced via the calculation of particle trajectories [Eq. (15)]. We now have a set of equations to integrate for Q, M, D and F, which depends on Q, M, D, F, Q_t and the atmospheric pressure and density. Because we have both initial conditions at z=0

$$Q = Q_I, M = M_I, D = D_I, F = 0, \tag{28}$$

and final conditions

$$D = 0, Q = Q_t, \tag{29}$$

at some unknown height z=z_t, we use a shooting method (Press et al. 1992), and treat Q_t as an additional dependent variable in the system. Again, for convenience, we introduce a new dependent variable x, such that

$$z = xS, \tag{30}$$

and x ranges from 0 to 1. S is the height of the radial intrusion at which the density deficit is zero. We then solve the set of equations:

$$\begin{aligned} &\frac{dQ}{dx} = S\frac{dQ}{dz}, \quad \frac{dM}{dx} = S\frac{dM}{dz}, \quad \frac{dD}{dx} = S\frac{dD}{dz} \\ &\frac{dF}{dx} = S\frac{dF}{dz}, \quad \frac{dQ_t}{dx} = 0, \qquad \frac{dS}{dx} = 0, \end{aligned} \tag{31}$$

with four boundary conditions at x=0, given by Eq. (28) and two boundary conditions at x=1 given by Eq. (29).

Results

We now consider the possible effects of particle recycling on an eruption column as predicted by the model. If the eruption initially forms a plume, then a radially spreading, particle-laden intrusion develops at some neutral height. Some of the particles falling from this intrusion may be re-entrained into the plume, and these cold, dense particles then reduce the buoyancy of the continuing plume. In some cases, this reduction of buoyancy may cause the momentum flux at some height in the column to fall to zero, triggering a transition to flow-forming behaviour.

We consider a model eruption with mass flux πQ_I=3×108 kg s^{-1}, and an initial speed just in excess of the critical speed at which a plume is able to develop. In Fig. 2, we compare profiles of speed, solid mass flux and solid mass fraction both for calculations that include and neglect particle recycling. Particle recycling has a strong effect on the speed of the plume, and substantially reduces the minimum speed at the top of the gas-thrust region, which, in this calculation, is located about 3 km above the source (Fig. 2a). If we were to reduce the initial speed of the eruption, this minimum speed would decrease to zero as we approach critical conditions for collapse. However, the amount of solid material entrained

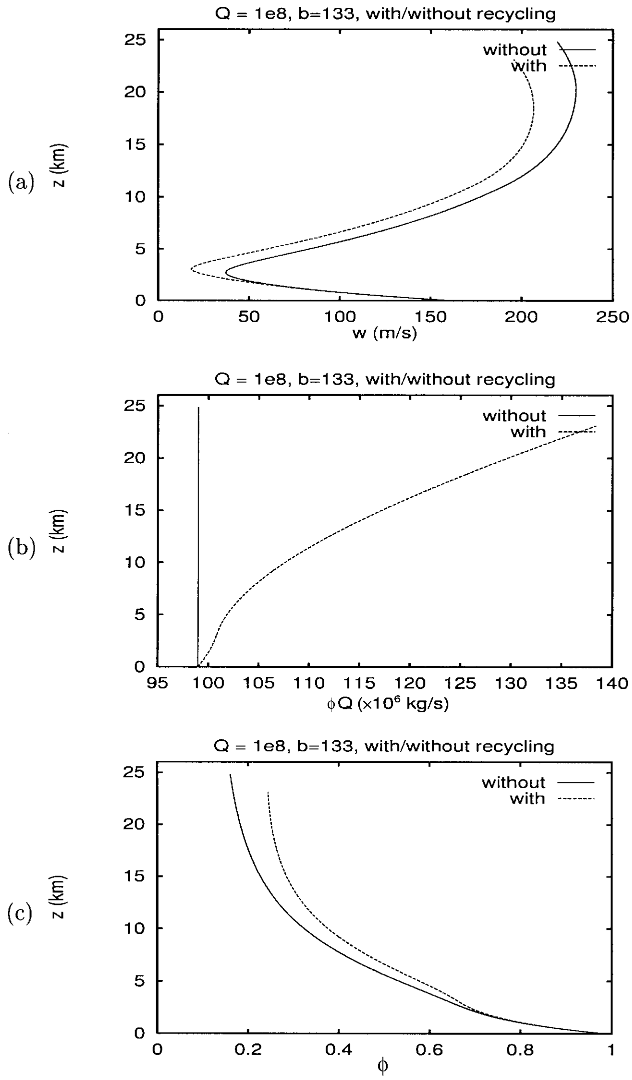

Fig. 2a–c Profiles of **a** speed, **b** solid mass flux, **c** mass fraction of solid in the plume as functions of height. Profiles are plotted for point *A* on Fig. 3, with initial mass flux πQ_I=3×10^8 kg s^{-1}, and an initial speed just above the critical speed for plume formation. On each figure, profiles are plotted for plumes with and without particle recycling

in the gas-thrust region, below z≈3 km, is small, as shown by the small increase in the solid mass flux in the plume below this height (Fig. 2b). Therefore, we expect that the increase in critical speed between the recycling and non-recycling cases will be relatively small compared with the actual speed, although we show in the Discussion and conclusions that this may play a key role in the formation of interleaved flow and fall deposits if the eruption rate increases through the threshold for collapse. Indeed, Fig. 3 compares the minimum speed required in order that a steady plume can develop as a function of the initial mass flux, both for models that include and neglect the effect of particle recycling. In the recycling calculation, we examine the limit of large particles (>80 μm in diameter) that fall with inertial drag. The model calculations correspond to plumes with an

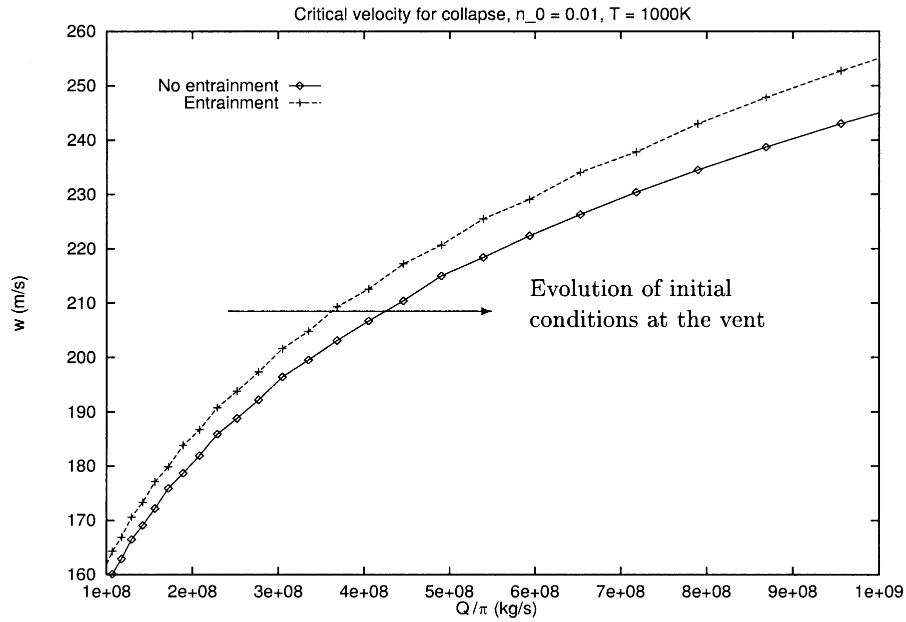

Fig. 3 Calculated values of the critical initial speed that an eruption must exceed to form a buoyant plume, as a function of the initial mass flux Q_I of the eruption. *Curves plotted* are for plumes that do not recycle particles, and for plumes that recycle particles falling with inertial drag. Particle recycling increases the critical speed for formation of a buoyant plume. The *arrow* indicates the evolution of the initial conditions at the vent in an eruption *i*, which the mass flux increases (see Discussion and conclusions)

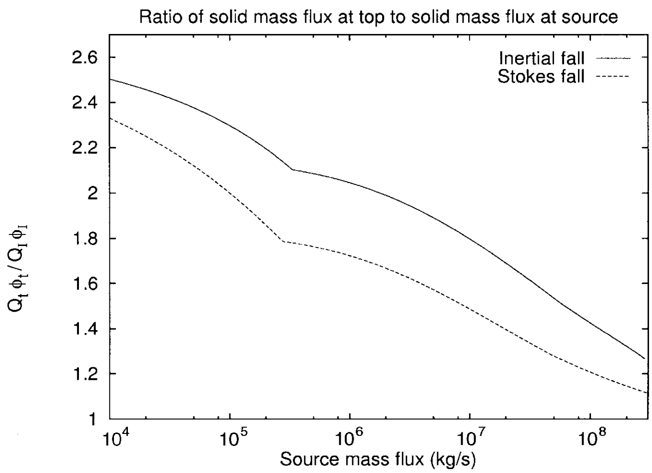

Fig. 4 Plot showing the fractional increase in solid mass flux from the bottom to the top of the plume, as a function of initial mass flux. The enhancement of the solid mass flux decreases as the initial mass flux and the plume height increase

initial temperature of 1,000 K and an initial mass fraction of gas 1% (corresponding to $ø_I$=0.99). The effect of particle recycling on the critical speed has a greater effect as πQ_I increases. For a given mass flux, the increase in the critical velocity may be as large as 5%, so that the fluctuations reported are most significant near the source.

Veitch and Woods (2000) showed that, for an incompressible laboratory scale plume, the fractional increase in particle increase from source to top is $e \approx 2.71$. However, for a compressible plume, this result is modified (see the section Fallout) because the total solid mass flux entrained decreases. Indeed, we have calculated the fractional increase in solid mass flux as a function of mass eruption rate. We find that the fractional increase is greatest for small mass eruption rates, when the variation in plume density with height is small. In Fig. 4, we plot the fractional change in solid mass flux for plumes with initial mass fluxes from $Q_I=10^4$ kg s^{-1} to $Q_I=3\times 10^8$ kg s^{-1}, for the limiting cases where particles all fall subject to Stokes or inertial drag. These results assume that a steady plume is sustained for several times longer than the recycling time-scale, to allow the re-entrainment process to reach a steady state. The recycling time will be dominated by the fall time, which for a 10-km plume will be around 1,000 s, or 20 min. Therefore, we expect a recycling plume to take an hour or more to reach a steady state; shorter eruptions will not reach this equilibrium.

Discussion and conclusions

The mass eruption rate of a number of volcanic eruptions (Wilson and Walker 1985; Carey and Sigurdson 1987) is believed to have increased over the course of the eruption as the conduit eroded and widened (Wilson et al. 1980). Woods and Bower (1995) have shown that, for simple conical vent geometry, the velocity of the decompressed jet that develops above the vent is primarily dependent on the magma temperature and volatile fraction, and only weakly dependent on the mass flux. Therefore, these eruptions may cross the critical curve from plume-forming to flow-forming behaviour as the mass eruption rate increases (Wilson et al. 1980). This evolution is represented by the arrow on Fig. 3. We sketch the possible evolution of the mass eruption rate and corresponding eruption regime in Fig. 5. The critical mass flux for the transition between plume-forming and flow-forming behaviour for a non-recycling plume is denoted Q_{CN}, and the critical mass flux for the breakdown of the steady solution for a recycling plume is denoted Q_{CE}.

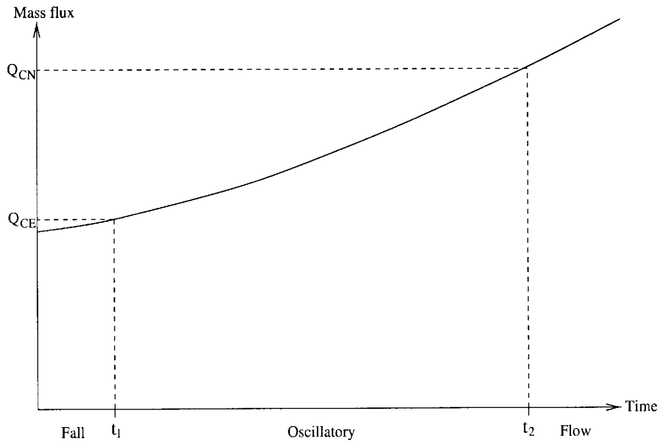

Fig. 5 Sketch of the increase in source mass flux with time. This may occur as the material in the walls of the conduit is eroded, and the vent widens (Wilson et al. 1980). At early times, the mass flux is small, and the eruption will form a plume. At later times, when the mass flux is large, the eruption will collapse as a pyroclastic flow. In the intermediate regime, particle recycling may cause the eruption to oscillate between the two forms of behaviour

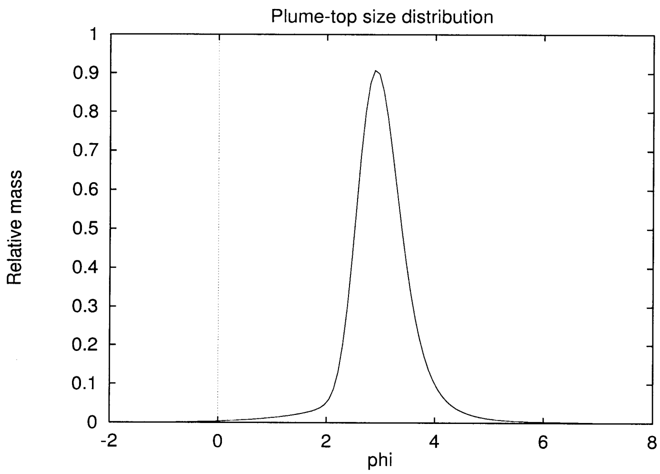

Fig. 6 The mass-weighted size distribution of particles at the top of the plume. The particle sizes are measured in ø-units, where ø is related to the diameter d in millimetres by $d=2^{-ø}$. This distribution is used to calculate fall speeds and deposit thicknesses

The mass eruption rate is initially low enough that the eruption forms a convecting plume. However, as the mass flux reaches Q_{CE} at time t_1, we move into a regime where the plume can not remain stable because of the re-entrainment of particles (cf. the experiments of Veitch and Woods, 2000). If the rate of increase of the mass flux is sufficiently slow then the eruption column may fluctuate between plume-forming and flow-forming behaviour. We envisage that beyond this time, t_1, the plume height begins to fall as solid particulate is recycled. Eventually, the column collapses when the amount of material entrained prevents the fluid–particle mixture in the lower gas-thrust region from becoming buoyant. The cycle then repeats, with the plume becoming re-established, and with the plume height increasing with eruption rate. However, once the mass eruption rate has increased beyond Q_{CN} at time t_2, the flow from the vent never becomes buoyant, and steady pyroclastic flows are formed.

Table 2 Times required to produce fall deposit layers of thicknesses 1 and 10 cm at distances 10 and 100 km from the vent. The eruption mass flux is 10^8 kg s^{-1}, and the particle size distribution at the plume top is as shown in Fig. 6

Thickness (cm)	Radial distance (km)	Source mass flux (kg s^{-1})	Time
1	10	10^8	25 min
1	100	10^8	82 min
10	10	10^8	4.1 h
10	100	10^8	13.6 h

We conclude that particle recycling may result in the height of a volcanic eruption column fluctuating in time if the recycling time is less than the time-scale for variation of the source eruption conditions.

The deposits from several eruptions show interleaved layers resulting from alternation between fallout from high Plinian columns and deposition from pyroclastic flows (Walker and Croasdale 1971; Wilson and Walker 1985; Carey and Sigurdsson 1987), and this interleaving has been attributed to periodic collapse of the eruption column (Wilson and Walker 1985). Although these studies do not provide enough information to infer the interval between recycling events, we can calculate the time required to form fall deposits of various thicknesses. We consider an example eruption with a source mass flux of $Q_I=10^8$ kg s^{-1} producing symmetrical deposits in a wind-free environment. The particle size distribution at the plume top is shown in Fig. 6. We assume that particle fall paths are described by Eqs. (13)and (14) (Sparks et al. 1991), and the void fraction in the fall deposit is taken to be 40%. The times required to produce fall deposits of thicknesses 1 and 10 cm at distances of 10 and 100 km from the vent using this fallout model are shown in Table 2. The time-scale to produce these layers ranges from around 20 min to a few hours, broadly in line with the estimated recycling time-scale discussed in the Introduction. Therefore, we conclude that particle recycling provides a possible mechanism for periodic plume collapse and the formation of interleaved flow and fall deposits seen in the field.

Particle recycling may also lower the height of the eruption column, by increasing the density of the plume, and lowering the neutral buoyancy height (Fig. 7). In Fig. 8, we plot the ratio of the neutral buoyancy height of the plume that recycles particles against the neutral buoyancy height of the plume that does not. We see that the fractional decrease in plume height is most significant when the mass eruption rate is large.

This change in height leads to possible errors in the estimation of the source mass flux using the approach of Wilson et al. (1978) and Settle (1978). In that method, the height is related to the mass flux by the buoyant plume theory of Morton et al. (1956), so that Q_I~H^4,

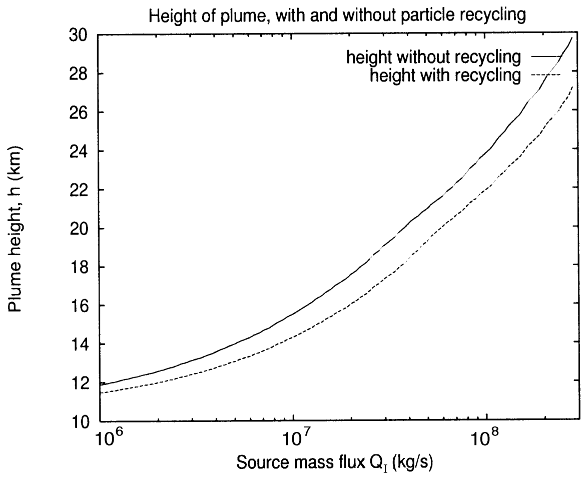

Fig. 7 The plume height is plotted against the initial mass flux Q_I, for recycling and non-recycling plumes. Particle recycling can reduce the height of the plume by as much as 10%

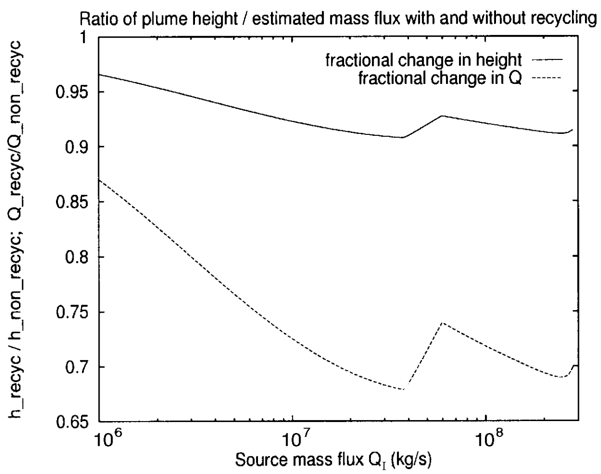

Fig. 8 Plots of the fractional reduction in plume height and estimated mass flux caused by recycling, as a function of mass flux. Particle recycling can reduce the height of the plume by as much as 10%, and the estimate of the mass flux by 35%

where H is the plume height. Therefore, a fractional change in column height, f, as a result of recycling, results in a change in the prediction of the associated mass flux Q_I proportional to f^4. Therefore if the classic plume theory approach is used to estimate the mass flux of a plume whose height has been reduced by 10% because of recycling, this will result in an underestimation of the mass flux by 35% (Fig. 8).

Although the calculations presented in this paper are somewhat idealised, they do identify some new and interesting features of particle fallout and the impact of particle–gas separation on the dynamics of volcanic eruption plumes and their deposits. In particular, they identify where the steady state assumption breaks down and where a plume that develops above a steady source behaves in an oscillatory fashion. In turn, we suggest this time-dependent behaviour may be associated with the formation of interleaved flow and fall deposits. One effect that may lead to further complexities concerns the aggregation of particles into accretionary lapilli in the plume (Gilbert and Lane 1994). In a further study (Veitch and Woods, in preparation), we show that this process has only a small impact on the results of the present study, but the formation of such lapilli leads to significant variation in the air-fall deposition patterns as a function of distance from the source, which is in accord with the data of Carey and Sirgurdsson (1982).

Acknowledgements We would like to thank the two anonymous referees of this paper who provided some valuable comments that led to improvements in the paper.

References

Anilkumar AV, Sparks RSJ, Sturtevant B (1993) Geological implications and applications of high-velocity two-phase flow experiments. J Volcanol Geotherm Res 56:145–160

Bursik MI, Sparks RSJ, Gilbert JS, Carey SN (1992) Sedimentation of tephra by volcanic plumes: I. theory and its comparison with a study of the Fogo A Plinian deposit, San Miguel (Azores). Bull Volcanol 54:329–344

Carey SN, Sigurdsson H (1982) Influence of particle aggregation on deposition of distal tephra from the May 18 1980 eruption of Mount St. Helens Volcano. J Geophys Res 87:7061–7072

Carey SN, Sigurdsson H (1987) Temporal variations in column height and magma discharge rate during the 79 A.D. eruption of Vesuvius. Geol Soc Am Bull 99:303–314

Carey SN, Sparks RSJ (1986) Quantitative models of the fallout and dispersal of tephra from volcanic eruption columns. Bull Volcanol 48: 109–125

Gilbert JS, Lane SJ (1994) The origin of accretionary lapilli. Bull Volcanol 56: 398–411

Kaye GWC, Laby TH (1973) Tables of physical and chemical constants and some mathematical functions, 14th edn. Longman, London

Martin D, Nokes R (1988) Crystal settling in a vigorously convecting magma chamber. Nature 332:534–536

Morton BR (1959) Forced plumes. J Fluid Mech 5:151–163

Morton BR, Taylor GI, Turner JS (1956) Turbulent gravitational convection from maintained and instantaneous sources. Proc R Soc Lond Ser A 234:1–23

Neri A, Dobran F (1994) Influence of eruption parameters on the thermofluid dynamics of collapsing volcanic columns. J Geophys Res 99:11833–11857

Press WH, Teukolsky SA, Vetterling WT, Flannery BP (1992) Numerical recipes in FORTRAN – the art of scientific computing, 2nd edn. Cambridge University Press, Cambridge

Ricou FP, Spalding DB (1961) Measurements of entrainment by axisymmetrical turbulent jets. J Fluid Mech 11:21–32

Settle M (1978) Volcanic eruption clouds and the thermal power output of explosive eruptions. J Volcanol Geotherm Res 3:309–324

Shapiro AF (1953) Dynamics and thermodynamics of compressible fluids. Ronald Press, New York

Sparks RSJ, Carey SN, Sigurdson H (1991) Sedimentation from gravity currents generated by turbulent plumes. Sedimentology 38:839–856

Sparks RSJ, Bursik MI, Carey SN, Gilbert JS, Glaze LS, Sigurdsson H, Woods AW (1997) Volcanic plumes. Wiley, New York

Turton R, Clark NN (1987) an explicit relationship to predict spherical particle terminal velocity. Powder Tech 53:127–129

Veitch G, Woods AW (2000) Particle recycling and oscillations of volcanic eruption columns. J Geophys Res 105:2829–2842
Walker GPL, Croasdale R (1971) Two Plinian-type eruptions in the Azores. J Geol Soc Lond 127:17–55
Wilson CJN, Walker GPL (1985) The Taupo eruption, New Zealand. 1. General aspects. Philos Trans R Soc Lond Ser A 314:199–228
Wilson L (1976) Explosive volcanic eruptions. III: Plinian eruption columns. Geophys J R Astron Soc 45:543–556
Wilson L, Sparks RSJ, Huang TC, Watkins ND (1978) The control of volcanic column height by eruption energetics and dynamics. J Geophys Res 83:1829–1836
Wilson L, Sparks RSJ, Walker GPL (1980) Explosive volcanic eruptions–IV. The control of magma properties and conduit geometry on eruption column behaviour. Geophys J R Astron Soc 63:117–148
Woods AW (1988) The fluid dynamics and thermodynamics of eruption columns. Bull Volcanol 50:169–193
Woods AW, Bower S (1995) The decompression of volcanic jets in craters. Earth Planet Sci Lett 131:189–205
Woods AW, Bursik MI (1991) Particle fallout, thermal disequilibrium and volcanic plumes. Bull Volcanol 53:559–570
Woods AW, Caulfield CCP (1992) A laboratory study of explosive volcanic eruptions. J Geophys Res 97:6699–6712